Electrical current-induced structural changes and chemical functionalization of carbon nanotubes

ARTICLE *in* JOURNAL OF APPLIED PHYSICS · NOVEMBER 2006

Impact Factor: 2.18 · DOI: 10.1063/1.2363816

Electrical current-induced structural changes and chemical functionalization of carbon nanotubes

S. Agrawal and M. S. Raghuveer
Materials Science and Engineering Department, Rensselaer Polytechnic Institute, Troy, New York 12180

R. Kröger
Institut für Festkörperphysik, Universität Bremen, Otto-Hahn-Allee 1, Bremen 28359, Germany

G. Ramanath[a)]
Materials Science and Engineering Department, Rensselaer Polytechnic Institute, Troy, New York 12180

(Received 9 May 2006; accepted 1 September 2006; published online 9 November 2006)

We demonstrate that high current densities, combined with air exposure can slice, weld, and chemically functionalize multiwalled carbon nanotubes (CNTs) with carboxyl and allyl moieties, and alter the electrical properties. The conductance of thin film assemblies of CNTs increases by 150%, indicating that the increase in the number of low-resistance pathways caused by CNT junction formation offsets the conductance decrease expected from defect creation, surface functionalization, and fissure. Such welded high-conductance CNT networks of functionalized CNTs could be useful for device and sensor applications, and may serve as high mechanical toughness mat fillers that are amenable to integration with nanocomposite matrices. © *2006 American Institute of Physics*. [DOI: 10.1063/1.2363816]

I. INTRODUCTION

Carbon nanotubes (CNTs) are promising materials for nanodevices due to their attractive optical, mechanical, and electronic properties arising from their unique molecular structure, geometrical shape, and electronic structure.[1] Many envisioned CNT-based applications such as device interconnections in integrated circuits require directed growth of aligned CNTs,[2] low-resistance high-strength CNT junctions[3] with tunable chemistry, stability, and electronic properties.[4] Significant progress has been made in directing the growth of CNT bundles[5] and utilizing them as interlayer interconnects.[6] However, forming CNT-CNT junctions on the substrate plane in a scalable fashion, to enable in-plane device circuitry and interconnections, remains to be realized. Even in small-scale test structures with overlapping CNTs created through nanoprobe manipulation and electrofluidic techniques, transforming the high contact resistance at overlapping CNTs to low-resistance CNT-CNT welds without destroying the CNT structure is a major challenge. Recent works have explored eV–keV range ion[7] or electron[8,9] beams to alter the structure, cut, weld, and chemically functionalize CNTs with nanoscopic lateral resolution[10] to tailor the electrical properties of CNTs and their assemblies. These techniques, however, require the positioning of the energetic beam at the exact location where welding or machining is desired.

Here, we show that electrical currents passed through a thin film comprised of randomly dispersed multiwalled CNTs can alter the structure, chemically functionalize, and tailor the electrical properties of CNTs. We demonstrate that application of current can cut, thin, weld CNTs, and functionalize them with carboxyl and allyl moieties when subject to air exposure. Additionally, the resistance of the CNT networks decreases due to the predominance of increase in the number of effective conduction paths enabled by the creation of CNT-CNT welds, offsetting the resistance increase due to defect creation and CNT fissures. Our results thus suggest that the structural stability of CNTs subjected to high current densities is dependent on the configuration, in which they are assembled, and can be much lower for networks with overlapping CNTs. Furthermore, the passage of electrical current may be an attractive strategy for creating mats comprised of interlinked networks of CNTs for creating in-plane CNT circuitry or use as high-toughness mechanical reinforcements in composites.

II. EXPERIMENTAL DETAILS

Multiwalled CNTs synthesized by arc discharge[11] were used for our experiments. We drop coated a film comprised of randomly dispersed CNTs over lithographically patterned 100-nm-thick Au pads on oxidized silicon substrates. The Au contact pads patterned by a lift-off technique were used to serve as low-resistance contacts for four point probe measurements, as reported elsewhere.[12] A 50-nm-thick Cr layer was deposited prior to Au deposition to provide enhanced adhesion with the silica surface. Four point probe *I-V* measurements were carried out using a Keithley 2400 sourcemeter and a Keithley 2000 multimeter in $\sim 10^{-7}$ Torr vacuum. Currents in the range of 0.1–1 A were applied into the thin film CNT samples. The films were characterized in both plan-view and edge-on configurations by scanning electron microscopy (SEM) using a JEOL 6330F FESEM instrument operated at 5 kV. The structural changes in the CNTs were investigated by transmission electron microscopy (TEM) in Philips CM 12 and CM 20 instruments operated at 120 and 200 kV, respectively, with the latter providing 0.19 nm

[a)]Electronic mail: ramanath@rpi.edu

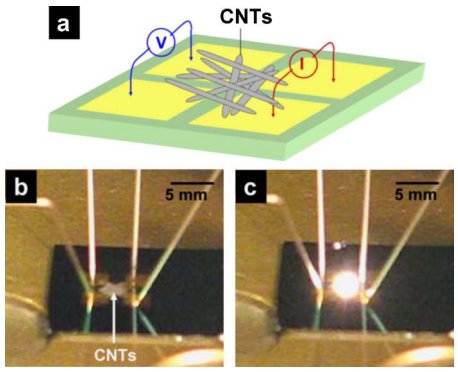

FIG. 1. (Color online) (a) Schematic sketch of a CNT film drop coated over Au pads for four-point-probe conductance measurements. Optical photographs of the CNT film contacted with four probes on the gold pads (b) before current exposure and (c) during application of 0.1–1 A current in air, capturing a momentary flash.

point-to-point resolution. The chemical changes in the CNTs were studied by Raman spectroscopy using a Renishaw Ramanscope system with a 514 nm argon laser, and Fourier transform infrared (FTIR) spectroscopy in a Nicolet Magna 560-FTIR tool in transmission mode.

III. RESULTS AND DISCUSSION

A. Current-induced flashes

Figure 1(a) shows a schematic sketch of the test architecture which consists of a film of multiwalled CNTs drop coated over Au contacts. Applying large currents between 0.1 and 1 A through the CNT films results in a series of momentary flashes of light followed by circuit breakdown. While the order-of-magnitude variability in the current at which the flashes are observed is likely due to variations in film homogeneity in different samples, currents $<\sim 100$ mA did not produce such flashes or result in breakdown in any of the samples investigated. Figures 1(b) and 1(c) show snapshots of the test structure and the flash generated during current application (also see supplemental video[32]). Carrying out similar experiments with $\sim 0.1-1$ A current in *a* $\sim 10^{-7}$ Torr vacuum results in a sustained glow emerging from the CNTs, as reported earlier,[13] but suppresses electrical breakdown. The critical current density above which the flashes are observed is estimated to be 10^5-10^7 A cm^{-2}, based on the nanotube density in the film estimated by analysis of SEM images.[14] This current density is two to four orders of magnitude smaller than the 10^9 A cm^{-2} current densities that can be sustained in individual CNTs.[15]

B. Structural and morphological changes

SEM analyses reveal that applying 0.1–1 A current results in structural and morphological changes in the CNT films [see Figs. 2(a) and 2(b)]. No observable changes are seen for $<\sim 100$ mA, when no flashes were observed, indicating that the morphological changes are related to the flashes. Figure 2(b) illustrates the examples of current-induced welding of overlapping CNTs (see arrows). TEM micrographs from samples subjected to high current densities confirm the formation of CNT welds [see Fig. 2(c)]. At the

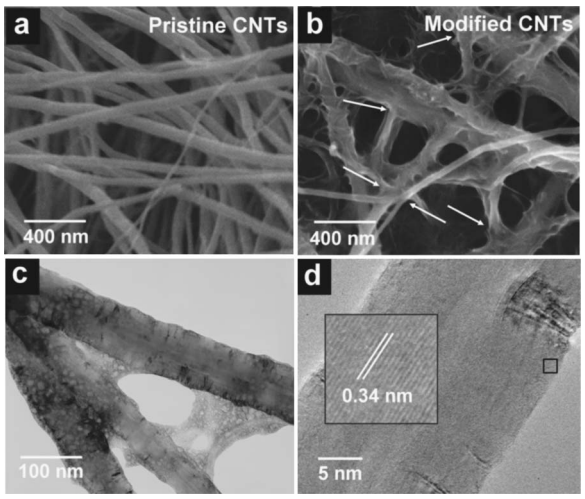

FIG. 2. Representative SEM images from a CNT film (a) before and (b) after 0.1–1 A current application. Current-induced CNT-CNT joints are indicated by arrows. Representative TEM images show close-up views of (c) a CNT-CNT weld held together by amorphous carbon bridges, and (d) a large diameter (~ 100 nm) CNT with the hollow intact. The inset shows that the crystallinity is preserved after current modification.

CNT welds, we observe a coating of amorphous carbon that is presumably deposited from carbon flux from electromigration, thinning[16,17] and rupture of smaller diameter CNTs present in the neighborhood (see below). The amorphous carbon coating is analogous to the coating of a feed material used in metal joining,[18] and is different from current-induced spot welding observed in single walled CNTs where no amorphous carbon formation is observed.[19] The crystalline structure along the length of the CNT is, however, preserved in regions away from the welds, as illustrated in Fig. 2(d), indicating that the structural changes can be restricted to the CNTs joints. In some instances, we also observe graphitic carbon onions [see Fig. 3(a)], mainly on Fe nanoparticles, suggesting that the remnant catalysts promote onion formation.[20–22] Many CNTs are either thinned or ruptured near the welds [see Figs. 3(b) and 3(c)], likely by vaporization and electromigration of carbon atoms, induced by high current densities, and resultant joule heating. In locations where only a few CNTs bridge different portions of the sample, the CNTs tend to align, likely due to the effect of high local electric fields,[23] prior to rupture [see Figure 3(d)]. All the observed morphological changes are observed in experiments conducted in vacuum, or in air, suggesting the negligible effect of these ambients on current-induced structural changes.

Current-induced structural changes of CNTs can be understood as follows. The high CNT-CNT resistance due to the lack of direct electron transport pathways across overlapping CNTs (Ref. 24) facilitates welding by joule heating and arcing induced by high currents at points proximal to the overlap. Additionally, catalyst particles and locations of Stones-Wales-type[25] defects on the CNTs could also serve as hot spots. The nature of the structural change, e.g., welding versus fissure, is likely to be determined by many factors such as CNT diameter, local current density, and distance from the next CNT, similar to ion-beam-induced structural changes.[7]

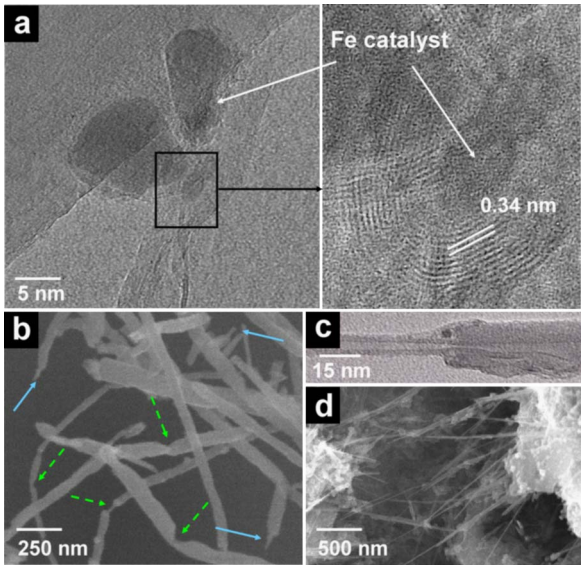

FIG. 3. (Color online) (a) TEM image of carbon onions on Fe catalyst nanoparticles near the weld site. The inset shows crystalline structure of a carbon onion. (b) SEM image showing thinning and rupture of CNTs shown by dashed green and solid blue arrows, respectively. (c) TEM image of a thinned down CNT. (d) SEM image showing alignment and rupture of CNTs.

C. Chemical functionalization

Raman and FTIR spectroscopies show that high current densities lead to the creation of defects such as vacancies and dangling bonds in CNTs, which upon air exposure result in the functionalization of the CNT surfaces. In particular, the ratio between the intensities of the D (1360 cm^{-1}) and G (1584cm^{-1}) bands increases from 0.20 to 0.35 upon applying ~0.1–1 A current. This result, summarized in Fig. 4(a), indicates an increase in sp^3 carbon, signifying an increase in the extent of disorder in the CNTs due to the creation of Stones-Wales-type defects and out-of-basal-plane dangling bonds. Upon air exposure, these defects sites serve as fertile high-reactivity sites for the formation of O–H, O═C–OH, C═O, and C═C moieties on the CNT surfaces via reaction with oxygen and moisture. Figure 4(b) shows representative FTIR spectra from CNT films subject to the application of ~0.1–1 A current and subsequently exposed to air. The characteristic signatures of hydroxyl, carboxyl, carbonyl, and allyl moieties are clearly seen at ~3440, 1710, 1640, and 1540 cm^{-1}, respectively. In contrast, pristine CNTs do not show any detectable signatures of these moieties. We therefore infer that current application combined with air exposure functionalizes the CNTs near the hot spots where dangling bonds have been created. The functionalization of CNTs with hydrophilic groups (e.g., carboxyl groups) in selected locations (e.g., at the welds) is attractive from the viewpoint of designing chemical and biological sensors using CNTs.

D. Electrical properties

Conductance-voltage (σ-V) characteristics obtained by four-point-probe measurements during the application of current reveal a monotonic irreversible increase in σ by ~150%, followed by saturation [see Fig. 5(a)]. The conductance gradient $d\sigma/dt>0$ and is the highest for the first minute of current application [see Fig. 5(b)], indicating that most of the structural and chemical changes occur during this time frame. The net increase in conductance is contrary to the reverse trend expected from defect creation, fissures, and functionalization of the CNTs. This observation indicates that the increase in the number of high-conductance path-

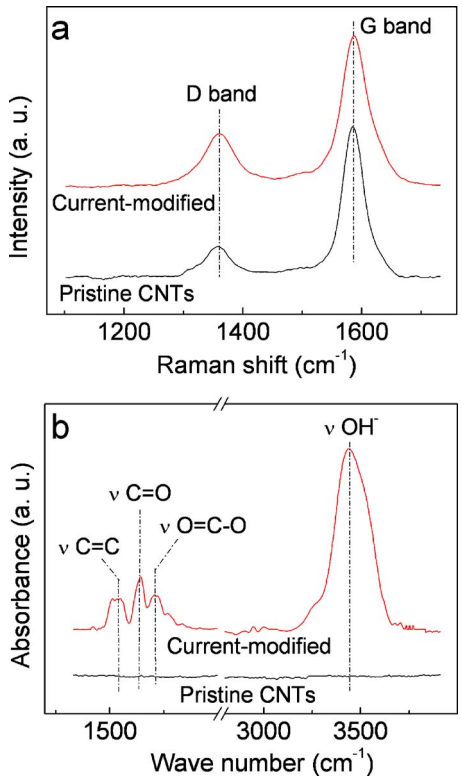

FIG. 4. (Color online) (a) Raman spectra of CNTs showing an increase in the D- to G-band intensity ratio upon current application. (b) FTIR spectra revealing CNT functionalization upon current application in air, in contrast to the featureless spectrum from pristine CNTs. Current application in vacuum followed by air exposure yielded the same result.

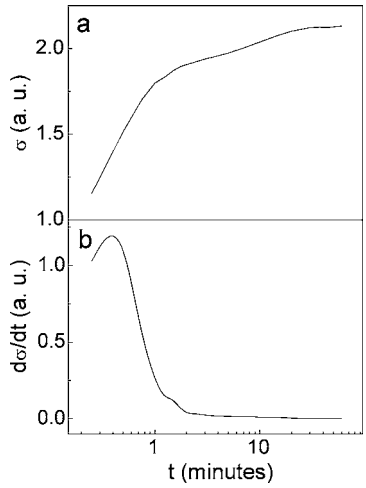

FIG. 5. Representative graphs capturing the changes in (a) the electrical conductance σ, normalized to the value measured at $t=0$, and (b) the rate of conductance change $d\sigma/dt$, as a function of time t, during the application of a constant current of 0.5 A into a film of randomly dispersed CNTs. Similar characteristics were obtained from other films applied with different current values in the range of 0.1–1 A.

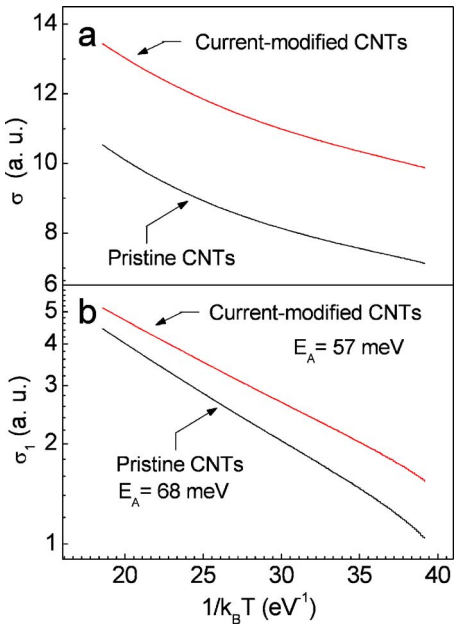

FIG. 6. (Color online) Variation of (a) total conductance σ and (b) thermally activated conductance component σ_1 as a function of temperature.

ways due to the formation of CNT-CNT junctions effectively offsets the conductance decrease expected from defect scattering, functionalization, and fracture of CNTs. We expect that multishell transport facilitated by the bridging of adjacent shells within each CNT,[26] and between CNTs (Ref. 27) at welds by dangling bonds, provide the mechanism for the observed conductance increase.

Figure 6(a) shows the electrical conductance of pristine and current-modified CNTs measured at different temperatures of $25\ ^\circ\mathrm{C} \leqslant T \leqslant 350\ ^\circ\mathrm{C}$. The behavior can be described by

$$\sigma = \sigma_0 \exp\left(-\frac{E_A}{k_B T}\right) + \sigma_2,$$

where the first term, designated as σ_1, reveals thermally activated transport across CNT shells, with an activation energy E_A.[28,29] We attribute the enhanced transport to the cross-linking of CNTs by the dangling bonds[30] created at the high current density hot spots. Current-induced bridging of CNTs decreases E_A slightly from 65 ± 5 to 50 ± 8 meV [see Fig. 6(b)]. Although the current applied to induce structural modification ranged from 0.1 to 1 A for different samples, the systematic current-induced decrease in E_A from pristine samples was reproducible in all of the ten samples studied. This result indicates that the current-induced change in conductance is insensitive to the actual configuration of the CNTs in randomly dispersed networks prepared by drop coating.

IV. CONCLUSIONS

Applying electrical currents to CNT films leads to structural modifications such as welding, thinning, rupture, and the chemical functionalization of CNTs with –COOH and –C═O groups. Current-induced welding increases the number of carrier transport pathways and increases the conductance by up to 150% and decreases the energy barrier for conduction, offsetting the decrease in conductance expected due to defect creation and CNT fissures. Current-induced conductivity enhancement at CNT-CNT contacts could be useful for creating mesoscale networks of device wiring with CNTs placed at specific locations by other techniques.[31] Apart from increasing the conductance, creation of welds could also improve the mechanical properties of CNT networks, and facilitate their use as high toughness reinforcers that are more amenable to integration with nanocomposite matrices.

ACKNOWLEDGMENTS

We gratefully acknowledge funding support from the National Science Foundation through Grant No. ECS 424322 and the NY state through the focus center.

[1] M. Ouyang, J. L. Huang, C. L. Cheung, and C. M. Lieber, Science **292**, 702 (2001).
[2] Q. Ngo, D. Petranovic, S. Krishnan, A. M. Cassell, Q. Ye, J. Li, M. Meyyappan, and C. Y. Yang, J. Comput. Neurosci. **3**, 311 (2004).
[3] S. Paulson, A. Helser, M. B. Nardelli, R. M. Taylor II, M. Falvo, R. Superfine, and S. Washburn, Science **290**, 1742 (2000).
[4] R. B. Capaz, C. D. Spataru, P. Tangney, M. L. Cohen, and S. G. Louie, Phys. Rev. Lett. **94**, 036801 (2005).
[5] B. Q. Wei, R. Vajtai, Y. Jung, J. Ward, R. Zhang, G. Ramanath, and P. M. Ajayan, Nature (London) **416**, 495 (2002).
[6] J. Li, Q. Ye, A. Cassell, H. T. Ng, R. Stevens, J. Han, and M. Meyyappan, Appl. Phys. Lett. **82**, 2491 (2003).
[7] M. S. Raghuveer, P. G. Ganesan, J. D'Arcy-Gall, G. Ramanath, M. Marshall, and I. Petrov, Appl. Phys. Lett. **84**, 4484 (2004).
[8] A. Kis *et al.*, Nat. Mater. **3**, 153 (2004).
[9] M. Terrones, F. Banhart, N. Grobert, J. C. Charlier, H. Terrones, and P. M. Ajayan, Phys. Rev. Lett. **89**, 075505 (2002).
[10] M. S. Raghuveer, A. Kumar, M. J. Frederick, G. P. Louie, P. G. Ganesan, and G. Ramanath, Adv. Mater. (Weinheim, Ger.) **18**, 547 (2006).
[11] T. W. Ebbesen and P. M. Ajayan, Nature (London) **358**, 220 (1992).
[12] Z. Yao, C. L. Kane, and C. Dekker, Phys. Rev. Lett. **84**, 2941 (2000).
[13] J. Q. Wei, H. W. Zhu, D. H. Wu, and B. Q. Wei, Appl. Phys. Lett. **84**, 4869 (2004).
[14] SEM observations over more than 20 regions reveal an average of 13.5 ± 7.7 CNTs in each μm^2 aerial segment, yielding a CNT density of $\sim10^9$ cm^{-2}, if we assume an isotropic distribution of CNTs. Therefore, the number of CNTs that intersect an $\sim10^{-3}$ cm^2 cross-section area (the sample cross section) are $\sim10^6$. For a mean CNT diameter of 30 nm, the total cross-sectional area of CNTs that contribute to transport is $\sim10^{-5}$ cm^2, which corresponds to $\sim10^4$–10^5 cm^{-2} current densities for 0.1–1 A currents, if all CNTs contribute to carrier transport. Since all CNTs are unlikely to be involved in carrier transport, the average current density would be higher, probably in the range of $\sim10^5$–10^7 A cm^{-2}.
[15] H. Dai, E. W. Wong, and C. M. Lieber, Science **272**, 523 (1996).
[16] J. Cumings, P. G. Collins, and A. Zettl, Nature (London) **406**, 586 (2000).
[17] P. G. Collins, M. Hersam, M. Arnold, R. Martel, and P. Avouris, Phys. Rev. Lett. **86**, 3128 (2001).
[18] Z. Sun and M. Kuo, J. Mater. Process. Technol. **87**, 213 (1999).
[19] H. Hirayama, Y. Kawamoto, Y. Oshima, and K. Takayanagi, Appl. Phys. Lett. **79**, 1169 (2001).
[20] R. S. Ruoff, D. C. Lorents, B. Chan, R. Malhotra, and S. Subramoney, Science **259**, 346 (1993).
[21] F. Le Normand, L. Constant, G. Ehret, M. Romeo, A. Charai, W. Saikaly, and C. Speisser, Philos. Mag. A **79**, 1739 (1999).
[22] F. Banhart and P. M. Banhart, Adv. Mater. (Weinheim, Ger.) **9**, 261 (1997).
[23] X. Q. Chen, T. Saito, H. Yamada, and K. Matsushige, Appl. Phys. Lett. **78**, 3714 (2001).
[24] M. Stadermann, Phys. Rev. B **69**, 201402(R) (2004).
[25] A. J. Stone and D. J. Wales, Chem. Phys. Lett. **128**, 501 (1986).
[26] J. A. V. Pomoell, A. V. Krasheninnikov, K. Nordlund, and J. Keinonen, J.

Appl. Phys. **96**, 2864 (2004).
[27]A. J. R. da Silva, A. Fazzio, and A. Antonelli, Nano Lett. **5**, 1045 (2005).
[28]S. Agrawal, M. J. Frederick, F. Lupo, P. Victor, O. Nalamasu, and G. Ramanath, Adv. Funct. Mater. **15**, 1922 (2005).
[29]P. G. Collins and P. Avouris, AIP Conf. Proc. **633**, 223 (2002).
[30]C. Miko, M. Milas, J. W. Seo, E. Couteau, N. Barisic, R. Gaal, and L. Forro, Appl. Phys. Lett. **83**, 4622 (2003).
[31]Y. M. Wang, W. Q. Han, and A. Zettl, New J. Phys. **6**, 15 (2004).
[32]See EPAPS Document No. E-JAPIAU-100-224621 for a video showing momentary flashes on passing ~1 A current through the CNT film in air. A stable glow is observed on doing a similar experiment in 10^{-7} Torr vacuum. This document can be reached via a direct link in the online article's HTML reference section or via the EPAPS homepage (http://www.aip.org/pubservs/epaps.html).